From Industrially Weavable and Knittable Highly Conductive Yarns to Large Wearable Energy Storage Textiles

Yan Huang,[†] Hong Hu,[‡] Yang Huang,[†] Minshen Zhu,[†] Wenjun Meng,[†] Chang Liu,[‡] Zengxia Pei,[†] Chonglei Hao,[∞] Zuankai Wang,[∞] and Chunyi Zhi*[,†,§]

[†]Department of Physics and Materials Science, City University of Hong Kong, 83 Tat Chee Avenue, Hong Kong, China, [‡]Institute of Textiles and Clothing, The Hong Kong Polytechnic University, 11 Hong Chong Road, Hong Kong, China, [∞]Department of Mechanical and Biomedical Engineering, City University of Hong Kong, 83 Tat Chee Avenue, Hong Kong, China, and [§]Shenzhen Research Institute, City University of Hong Kong, Shenzhen 518000, China

ABSTRACT Wearable electronic textiles that store capacitive energy are a next frontier in personalized electronics. However, the lack of industrially weavable and knittable conductive yarns in conjunction with high capacitance, limits the wide-scale application of such textiles. Here pristine soft conductive yarns are continuously produced by a scalable method with the use of twist-bundle-drawing technique, and are mechanically robust enough to be knitted to a cloth by a commercial cloth knitting machine. Subsequently, the reduced-graphene-oxide-modified conductive yarns covered with a hierarchical structure of MnO_2 nanosheets and a polypyrrole thin film were used to fabricate weavable, knittable and wearable yarn supercapacitors. The resultant modified yarns exhibit specific capacitances as high as 36.6 mF cm^{-1} and 486 mF cm^{-2} in aqueous electrolyte (three-electrode cell) or 31 mF cm^{-1} and 411 mF cm^{-2} in all solid-state two-electrode cell. The symmetric solid-state supercapacitor has high energy densities of 0.0092 mWh cm^{-2} and 1.1 mWh cm^{-3} (both normalized to the whole device) with a long cycle life. Large energy storage textiles are fabricated by weaving our flexible all-solid-state supercapacitor yarns to a 15 cm × 10 cm cloth on a loom and knitting in a woollen wrist band to form a pattern, enabling dual functionalities of energy storage capability and wearability.

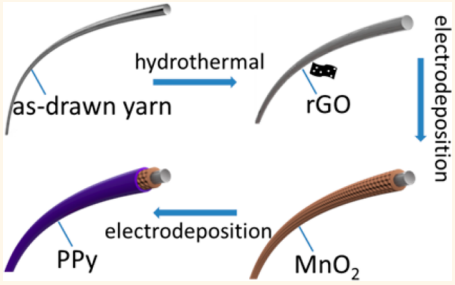

KEYWORDS: energy storage textiles · yarn supercapacitors · weavability · knittability · wearability

Wearable energy storage textiles are a representative advance in personalized electronics.[1−4] The supercapacitors in the form of yarn-based wearable pads are in particular one important category of such textiles for their high power density, fast rate of charge−discharge and long cycling lifetime as well as good compatibility with traditional textiles.[5−9] However, although some yarn-supercapacitors-based textiles have been demonstrated, appropriate fiber-building materials are still being searched to function both as active supercapacitor electrodes and as weavable, knittable, and wearable yarns by weaving and knitting machines.[1] In addition, although conventionally nonconductive yarns and textiles have been converted to be conductive by repetitive surface coating of carbon nanotubes (CNTs)[10−15] and metals,[16] such multistep fabrications give rise to cost-expensive and time-consuming limitations,[17] as well as pattern diversity challenges when the textiles are coated. As an alternative approach, carbon materials (*e.g.*, CNTs, graphene, reduced graphene oxide (rGO)) have been made to fibers and yarns for potential wearable applications.[5,18−27] However, on one hand, a constraint of these carbonaceous materials lies in their low capacitance. More importantly, a desirable feature possibly missed in these yarns is the weavability and knittability by commercial weaving and knitting machines. These machines usually pose on an input tensile stress of 2−4 MPa on the weaving or knitting yarn, and even worse, such that the tensile stress drastically increases at an exponential rate at the weaving or knitting area due to friction among yarns and mechanical parts. This may finally induce fracture of the yarns. Thus, mechanically tough materials are required for practical weaving and/or knitting. More importantly, as Lee *et al.*[28] pointed out on *Science*, the effective long-distance electron transport

* Address correspondence to cy.zhi@cityu.edu.hk.

Received for review February 6, 2015 and accepted April 4, 2015.

Published online April 05, 2015
10.1021/acsnano.5b00860

required in the wire or yarn format can only be achieved with the use of metallic materials.

Conventional metallic wires give rise to weavability, knittability, and wearability challenges. However, it is found when the size of diameter scales down to micrometers, the case is different for some kinds of metals. In this paper, inspired by the fiber drawing technique widely used in the yarn fabrication industry, conductive yarns were continuously produced by twist-bundle-drawing multiple high-temperature-spun stainless steel 316L thin fibers together. The obtained large-scale-yield yarns have many advantages such as super strength, excellent conductivity, great corrosion resistance and thermal stability, as well as flexibility equivalent to common cellulose yarns. These yarns can be woven and knitted to soft clothes by industrial weaving and knitting machines without any difficulties. To achieve the goal of high capacitance, rGO, MnO_2, and polypyrrole (PPy) are deposited on the conductive yarns. Supercapacitors fabricated by the electrocapacitive materials-modified yarns show superior capacitances and energy densities without compromising power densities and cyclability. As a trial of weavable, knittable and wearable energy storage textiles, our flexible all-solid-state supercapacitor yarns are woven to a large cloth and knitted to a pattern in a woollen wrist band which effectively power a set of light-emitting diodes.

RESULTS AND DISCUSSION

Synthesis of PPy@MnO_2@rGO@Conductive Yarns. The twist-bundle-drawing technique is widely used to fabricate yarns in the industry. A bundle of thin 316L stainless steel fibers is twisted and drawn into yarns by a machine (FX-24, WEIJIN Spinning) for the large-scale production (an ultra fast yield rate of 0.2 m s^{-1}), as shown in Figure 1a. Stainless steel 316L is selected because its micrometer-sized fibers become very flexible, while in comparison, for example, 304 stainless steel microfibers are much more brittle. The low electric resistivity of as-drawn yarns (40 Ω/m) makes them serve as an excellent electrode substrate for long-distance electron transport. The twisted long yarns have a small diameter of 180−250 μm and are very soft and flexible as well (Figure 1b,c), comparable to those conventional cotton yarns. They exhibit much high tensile strength (over 700 MPa, Supporting Information Figure S1) and excellent weavability and knittability. An industrial 14 gauge STOLL electronic flat knitting machine posing tensile stress up to hundreds of MPa was used to knit these yarns to a cloth without any difficulty. The knitted cloth looks very similar to a cotton cloth (Figure 1d). These obtained conductive yarns can also suffer hand knitting in which carbon yarns always break (Supporting Information Figure 2). Benefited from the anticorrosion capability of 316L strainless steel, the obtained large-scale-yield yarns can withstand harsh conditions of high temperature and high vapor pressure without losing the high tensile strength, which makes it possible to grow various nanostructures on the yarns by many fabrication techniques. Metal oxides with different morphologies have been successfully grown on the yarns by different methods like electrodeposition, hydrothermal method and microwave synthesis. This greatly enhances the flexibility to utilize the conductive yarns for various applications.

MnO_2 and PPy were consecutively electrodeposited on the conductive yarns. Prior to the electrodeposition, GO was reduced to be rGO in the presence of NaOH and deposited onto the as-drawn conductive yarns by a hydrothermal method (Figure 1e). By doing so, we take advantage of synergistic effects as follows. First, the existence of rGO improves charge transfer of MnO_2 and also contributes to capacitance enhancement (Supporting Information Figure S3).[5,18] Second, NaOH not only reduces GO,[29] but also improves the wettability of pristine conductive yarns by introducing hydrophilic hydroxyl groups, which is generally used for the wettability improvement in the textile industry (Supporting Information Figure S4 and Supporting Information Videos 1 and 2). The improved wettability is important for the uniform aqueous electrodeposition of MnO_2 in the subsequent steps. It should be noted that arising from the great robustness of conductive yarns, which can suffer the harsh conditions of high temperature and high vapor pressure, they still maintain a good tensile strength close to that of pristine yarns after the hydrothermal treatment (Supporting Information Figure S1). Third, the electrodeposition to prepare high-capacitance MnO_2 can greatly enhance the capacitive performance.[30] Fourth, besides capacitance contribution, flexible PPy serves as a stress buffer during various deformations which are commonly faced by textiles.[31] The electrodeposition times of MnO_2 and PPy are optimized for the energy storage application (Supporting Information Figures S5 and S6). These synergistic effects are responsible for the high electrochemical performances observed from our hierarchical PPy@MnO_2@rGO-deposited conductive yarns.

Structural Characterization of Hierarchical Conductive Yarns. The uniform deposition and fully utilized ion-accessible surface area are beneficial for achieving high electrocapacitive performance. It can be seen that rGO, MnO_2 and PPy are all uniformly deposited on all tiny fibers of the conductive yarn due to the improved surface wettability mentioned above, as revealed by scanning electron microscopy (SEM).

Figure 2a shows that rGO ultrathin nanosheets have uniformly deposited. MnO_2 have a typical morphology of nanoflakes (Figure 2b). In contrast, a continuous thin film of PPy is uniformly electrodeposited on MnO_2, making the surface much smoother (Figure 2c). These as-prepared species are confirmed by Raman spectroscopy (Supporting Information Figure S7).

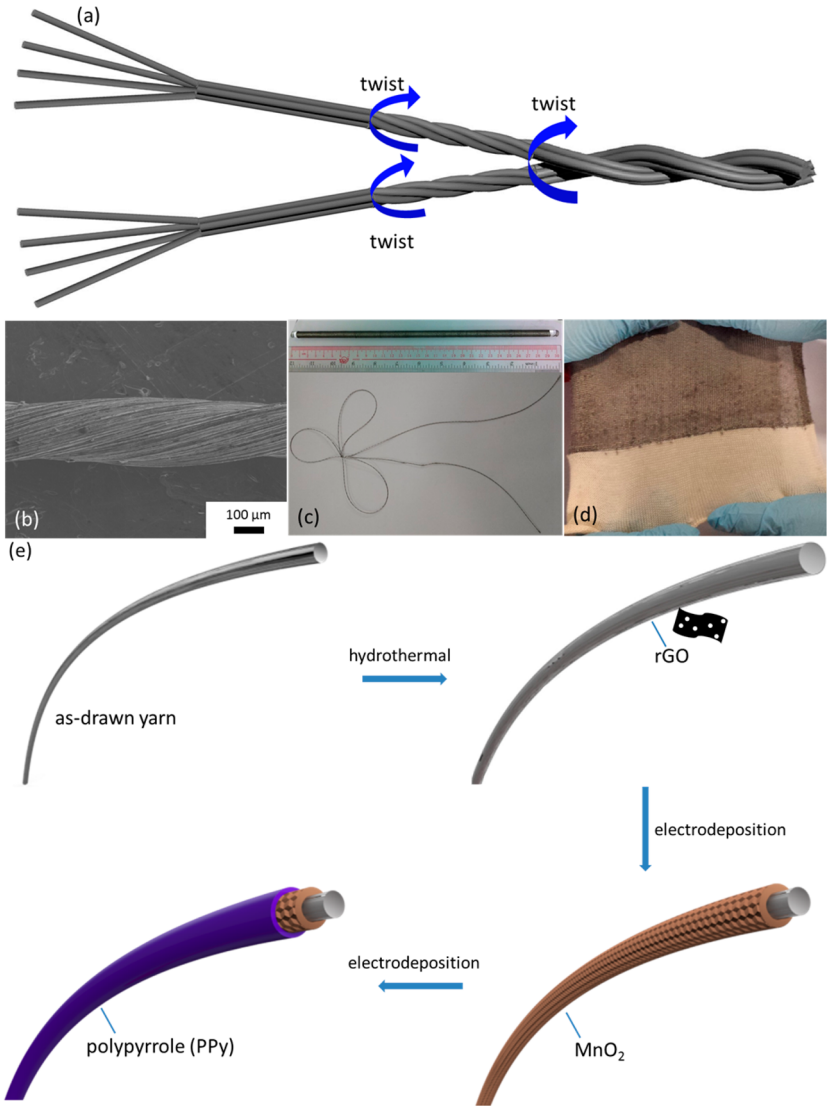

Figure 1. Schematics and demonstration of yarns. (a) Schematics of yarn fabrication. (b) Scanning electron microscopy (SEM) image of an as-drawn yarn. (c) A long yarn rolled on a rod and knotted. (d) A cloth knitted by the as-drawn yarn (gray-colored) and a cotton yarn (white-colored). (e) Illustration of the yarn modified by deposition of rGO, MnO_2 and PPy.

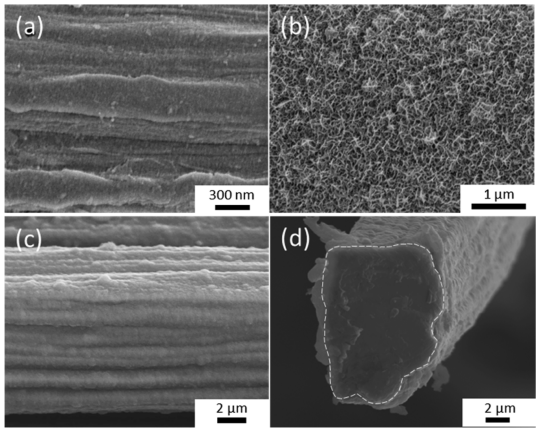

Figure 2. SEM characterization. (a) An rGO-deposited conductive yarn. (b) MnO_2 nanosheets. (c) PPy@MnO_2. Compared with the rough surface of MnO_2 nanosheets, the continuous PPy film makes the surface smoother. (d) Cross section of the PPy@MnO_2@rGO-deposited conductive yarn.

All these depositions result in a thin layer around 0.1 μm on the conductive fiber (Figure 2d). Such a thin layer of hierarchical structure is beneficial for fast ion transport during charge/discharge. Therefore, it is the one-dimensional thin PPy@MnO_2@rGO assemblies uniformly deposited on all available surfaces of tiny fibers that make our conductive yarns maximize the utilization of active capacitive materials and ion-accessible surface area which are attractive for high electrochemical performance supercapacitors.

Electrochemical Characterization of the Yarn Electrodes. We tested the electrochemical performance of the as-synthesized yarns in a three-electrode cell in Na_2SO_4. Their cyclic voltammetry (CV) curves at scan rates up to 500 mV s^{-1} and galvanostatic charge/discharge (GCD) curves at various current densities from 0.55 to 4.42 A cm^{-3} are shown in Figure 3a,b and Supporting Information Figure S10a. It should be noted that the

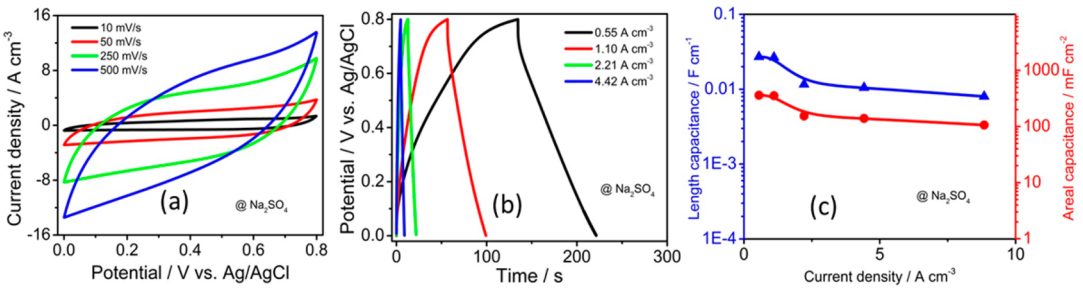

Figure 3. Electrochemical performance of the PPy@MnO_2@rGO-deposited conductive yarns in 1 M Na_2SO_4 measured in a three-electrode cell. (a) CV at various scan rates from 10 mV/s to 500 mV/s. (b) GCD at various current densities from 0.55 to 4.42 A/cm^3. (c) Specific length and areal capacitances with respect to current densities.

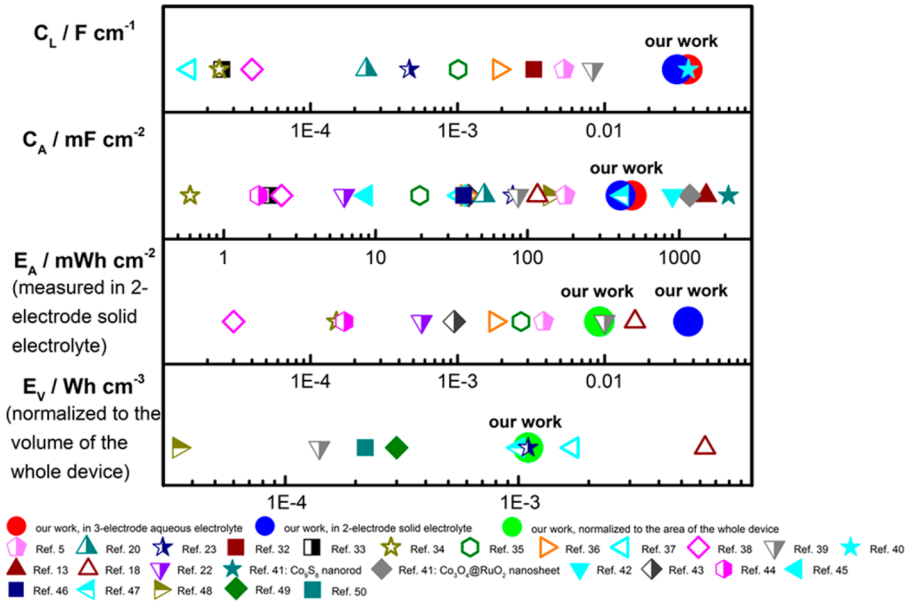

Figure 4. Comparison of electrochemical performance of various fiber/yarn-based electrocapacitive materials. Specific capacitances normalized to length (C_L) and area (C_A), and energy densities normalized to area (E_A) and volume (E_V).

scan rates and especially the current densities are much higher than most rates achieved for fiber/yarn-based supercapacitors.[5,18] This indicates the as-prepared yarns can endure very fast voltage/current change rates, which is believed to be a result of effective electrochemical dynamic processes in the hierarchical structure and the excellent conductivity of yarns. Specific capacitances normalized to length (C_L), area (C_A) and volume (C_V) of the yarn were calculated using CV curves (Supporting Information Figures S10b,c) and galvanostatic discharge curves (Figure 3c and Supporting Information Figure S10d). It can be seen that the hierarchical conductive yarn has specific capacitances of 36.6 mF cm^{-1} and 486 mF cm^{-2} in 1 M Na_2SO_4 in the three-electrode cell. To the best of our knowledge, these are the highest values, or at least close to them, of specific capacitances among all reported fiber-based supercapacitive materials (Figure 4 and Supporting Information Table S1).[5,13,18,20,22,23,32−50]

The observed high capacitances of the as-prepared yarns can be attributed to the synergistic effect in their uniformly deposited hierarchical structure associated with the fully utilized ion-accessible surface area of yarns, in which rGO improves charge transfer of MnO_2 and provides extra capacitance to the whole structure (Supporting Information Figure S3), MnO_2 contributes to the capacitance gain (Supporting Information Figure S5), and conducting PPy wrapped on the non-conductive MnO_2 provides a better conductivity for electron transportation and also participates in the pseudocapacitive charge storage process (Supporting Information Figure S6). Electrochemical impedance spectroscopy measurements (Supporting Information Figures S3b and S6b) show that the PPy@MnO_2@rGO-deposited conductive yarns have the smallest charge transfer resistance than those of the MnO_2@rGO-deposited conductive yarns and the MnO_2-deposited yarns (from the diameters of semicircles in the Nyquist plots), and a most vertical line at the end of the semicircular region. The multiple tiny fibers confined in a single yarn are uniformly wrapped with PPy@MnO_2@rGO and thus provide a large surface area for electrolyte penetration and ion transportation,

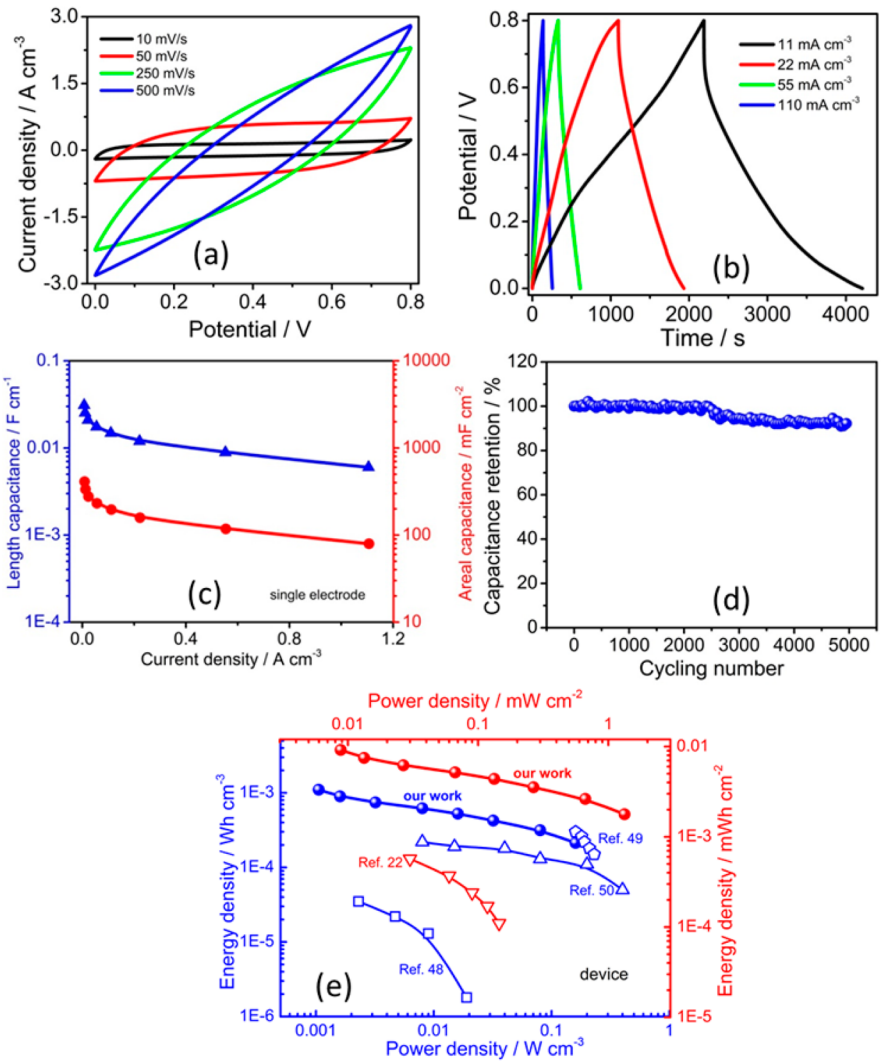

Figure 5. Electrochemical performance of the PPy@MnO_2@rGO-deposited conductive yarns measured in the two-electrode cell. (a) CV at various scan rates from 10 to 500 mV/s. (b) GCD at various current densities from 11 to 110 mA/cm^3. (c) Specific length and areal capacitances with respect to current densities. (d) Capacitance retention during charge/discharge cycles. (e) Ragon plot comparing areal/volumetric power and energy densities of MnO_2- and conducting polymer-based fiber/yarn supercapacitors.

therefore increasing the capacitances of yarns. The hydrophilicity pretreatment of pristine yarns using hydroxyl functional groups increases their surface wettability (small contact angle <10°, Supporting Information Figure S4 and Supporting Information Videos 1 and 2), which benefits the uniform depostion.

Electrochemical Characterization of All-Solid-State Yarn Supercapacitors. We used PPy@MnO_2@rGO-deposited conductive yarns as both active materials and current collectors to construct free-standing yarn supercapacitors. Typically, two parallel yarn electrodes were coated with poly(vinyl alcohol) (PVA)/H_3PO_4 electrolyte without binder or separator. Although the ionic conductivity in the solid electrolyte is much lower than that in the liquid, the yarn can still keep the CV shape at scan rates up to 500 mV s^{-1} (Figure 5a and Supporting Information Figure S11a) and be charged/discharged at current densities from 11 to 110 mA cm^{-3} with an almost triangular shape (Figure 5b and Supporting Information Figure S11b). The specific capacitances and energy density of a single-yarn electrode in the two-electrode test was calculated using galvanostatic discharge curves (Figure 5c and Supporting Information Figure S11c) to be 31 mF cm^{-1}, 411 mF cm^{-2} and 0.037 mWh cm^{-2} in solid-state PVA/H_3PO_4 electrolyte, outperforming most previously reported various yarn-based materials measured even in aqueous electrolytes (Figure 4 and Supporting Information Table S1). Figure 5d shows that the yarn supercapacitor retains over 92% of its initial capacitance after 4950 charge/discharge cycles at a high current density of 80 mA cm^{-3} (normalized to the whole device volume), demonstrating its impressive performance stability with a longer cycle life than reported PPy@MnO_2-based fibers and yarns.[13,51]

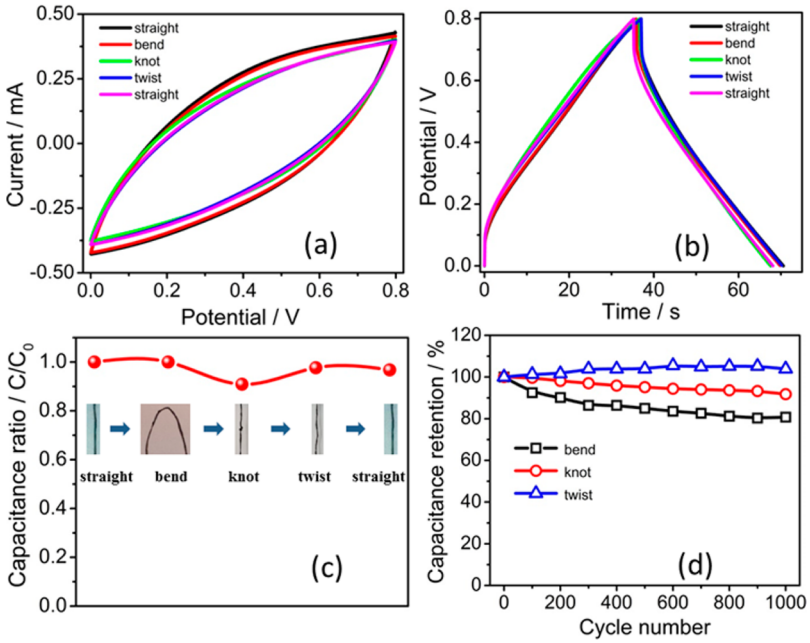

Figure 6. Flexibility tests of PPy@MnO_2@rGO-deposited conductive yarns measured in the two-electrode cell. (a) CV curves of the all-solid-state yarn supercapacitor undergoing consecutive deformations at a scan rate of 100 mV/s. (b) GCD curves of the all-solid-state yarn supercapacitor undergoing consecutive deformations at a current density of 80 mA/cm^3. (c) Capacitance ratio under various deformations. (d) Capacitance retention of the all-solid-state yarn supercapacitor after each deformation.

The volumetric/areal power and energy density normalized to the whole volume/area of the solid-state-supercapacitor is a meaningful parameter for the evaluation of the energy storage performance. The total volume and area of each yarn supercapacitor, including two yarns and the surrounding solid electrolyte, were estimated to be 0.00125 cm^3 and 0.15 cm^2, respectively. The areal energy density normalized to the total area of the whole device (0.0092 mWh cm^{-2}) outperforms most previously reported values normalized to the area of a single yarn electrode (Figure 4 and Supporting Information Table S1). The volumetric energy density of 1.1 mWh cm^{-3} is even comparable to that of microsupercapacitors (refs 23 and37, Figure 4 and Supporting Information Table S1). The Ragone plot in Figure 5e compares the volumetric and areal performance of our yarn supercapacitors to those of MnO_2- and conducting polymer-based fiber/yarn supercapacitors. To the best of our knowledge, the volumetric/areal energy and power density of our yarn supercapacitor are the highest values among all these fiber/yarn supercapacitors reported to date (Supporting Information Table S1).

To meet deformation stability needs for practical wearable applications, the yarn supercapacitor was further subjected to a consecutive deformation test, in the order of being straight, bent, knotted, twisted, and again straight. It can be seen from Figure 6a,b that there is only a slight change in these CV and GCD curves of the yarn supercapacitor subjected to a consecutive deformation. Figure 6c shows 100% and over 90% capacitance retention on bending to 90° and knotting, respectively. Upon twisting, capacitance retention increases to more than 97%, which is believed to result from the improved electrical contact, and therefore, the effectively reduced resistance by twisting, as in the case of stretch-induced conductivity[10] and capacitance enhancements.[31] After conforming to these complex nonplanar deformation tests, the yarn recovers to its original shape with over 96% of initial capacitance retained. Cycling test results under various mechanical deformations were shown in Figure 6d. It retains over 80%, 91% and 103% of initial capacitance after 1000 times under bending at 90°, knotting and twisting. All these reveal the excellent electrochemical stability and flexibility required for wearable electronics.

Weave, Knit, and Wear Energy Storage Textiles Made of High-Capacitance Yarns. To meet voltage and current needs for practical applications, five yarn supercapacitors were assembled both in series (Figure 7a,b) and in parallel (Figure 7c,d). Compared with a single yarn supercapacitor with an operating voltage of 0.8 V, the five-in-series assembly exhibits a 5-fold wider charge/discharge voltage window (4 V) with similar discharge time. The overall capacitance of the in-series assembly linearly decreases with the reciprocal of the number of yarn supercapacitors. Similarly, the current of the five supercapacitors connected in parallel increases by a factor of 5. The overall capacitance of the parallel assembly linearly increases with the number of yarn supercapacitors, suggesting a good scalability.

The combination of good flexibility and scalable assembly of high-capacitance yarns validates the

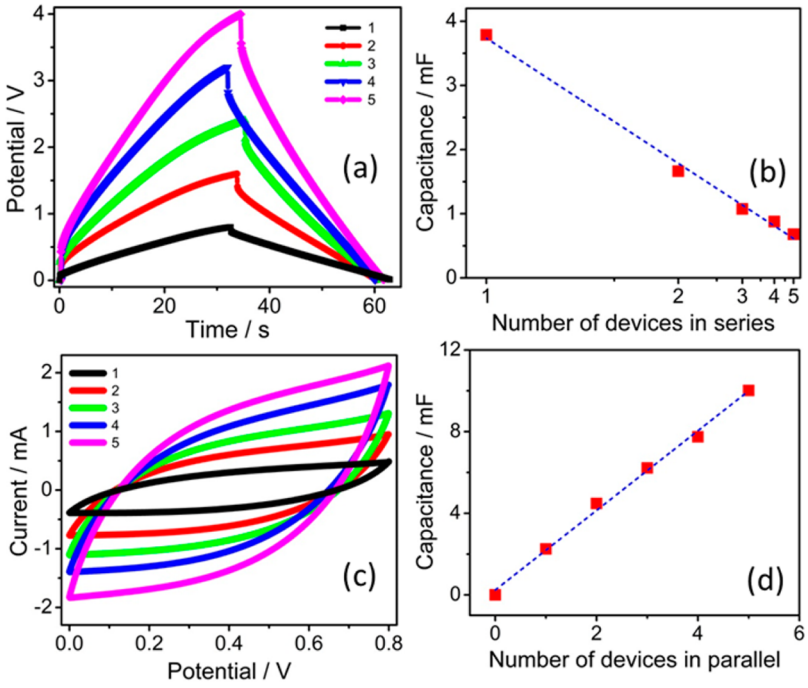

Figure 7. Electrochemical performance of multiple supercapacitors. (a) GCD at a current of 0.1 mA. (b) Capacitances in series with respect to the number of devices. (c) CV at scan rate of 100 mV/s. (d) Capacitances in parallel with respect to the number of devices.

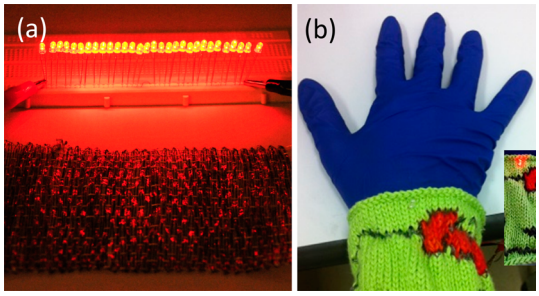

Figure 8. Photographs of the energy storage textiles made of yarns. (a) The 15 cm × 10 cm woven clothes can light 30 LEDs. (b) A wrist band knitted with a pattern (inset shows the pattern powering a LED).

application as energy storage textiles. For the first time, we used an AVL loom to weave a 15 cm × 10 cm clothes (Figure 8a) with a capacitance of 14 mF at the current of 5 mA by using 7 yarn supercapacitors in series (Supporting Information Figure S12). Moreover, we knitted a wrist band with a pattern by using the as-prepared yarns and common wollen yarns (Figure 8b). With the use of our soft yarns, pattern diversity can be easily realized with the use of the knitting technique. To the best of our knowledge, such weavability and knittability have never been reported before, not to mention the pattern diversity achieved in this work. Besides weavability, knittability and wearability, these fully charged energy storage textiles have been demonstrated to effectively power a set of light-emitting diodes, as shown in Figure 8a,b.

CONCLUSIONS

We have fabricated high-capacitance conductive yarns with hierarchical structures comprising deposited rGO, MnO_2, and PPy. With the use of the twist-spinning technique, pristine conductive yarns are continuously produced with a yield rate of 0.2 m s^{-1} and can be woven and knitted to clothes using industry-employed weaving and knitting machines. The resultant hierarchical structured yarns exhibit uniform deposition of electrocapacitive materials and large ion-accessible surface area, as is desirable for high-capacitance supercapacitors. These yarns show high specific capacities of 36.6 mF cm^{-1} and 486 mF cm^{-2} in aqueous Na_2SO_4 electrolyte (three-electrode cell), and 31 mF cm^{-1} and 411 mF cm^{-2} in solid-state PVA/H_3PO_4 electrolyte (two-electrode cell). A free-standing all-solid-state yarn supercapacitor made from two such parallel yarn electrodes using PVA/H_3PO_4 as the gelled electrolyte exhibits a long cycle life (more than 92% device capacitance retention over 4950 cycles), good flexibility and high energy densities of 0.0092 mWh cm^{-2} and 1.1 mWh cm^{-3} normalized to the whole device, which are much higher than most yarn-based supercapacitors normalized to the single electrode and even comparable to microsupercapacitors.

Our yarn supercapacitors can be assembled both in series and in parallel to meet the voltage and current requirements in practical application like energy storage textiles. A clothes has been woven and a wrist band with a pattern has been knitted, for the first time to our best knowledge. As a demonstration, these

energy storage textiles have been used to power a set of light-emitting diodes. The hierarchically structured conductive yarns and the yarn supercapacitors developed realize the weavability, knittability, wearability as well as pattern diversity. They could be regarded as a general architecture possessing great compatibility to modern textile industry for designing various wearable electronics.

EXPERIMENTAL SECTION

Synthesis of PPy@MnO_2@rGO−Deposited Conductive Yarns. Pristine conductive yarns were made of multiple tiny high-temperature-spun 316L stainless steel fibers by twist-drawing through a collaboration with Kezhengyuan Yarn Company. Then they were washed in acetone, ethanol and deionized water. GO was prepared from graphite flakes by a modified Hummers' method. Then, 0.25 mL GO aqueous solution (6 mg mL^{-1}) and 20 μL NaOH aqueous solution (1 M) were transferred in a Teflon-lined stainless steel autoclave (45 mL volume) containing a 10 cm as-spun conductive yarn and 20 mL deionized water. The mixed solution was heated at 180 °C for 12 h in an electric oven. The resultant yarns were electrodeposited with MnO_2 at 0.92 V *vs* Ag/AgCl for 45 min in a solution of 0.02 M manganese nitrate and 0.01 M sodium nitrate at room temperature, followed by PPy deposition at 0.8 V *vs* Ag/AgCl for 1.5 min in a solution of 0.1 M *p*-toluenesulfonic acid, 0.3 M sodium toluenesulfate, and 0.5% pyrrole monomer (v:v) at 0 °C. Prior to electrodeposition, pyrrole was distilled in order to purify pyrrole monomers.

Electrochemical Characterization of Individual Yarns. Capacitance measurements were performed in 1 M Na_2SO_4 aqueous electrolyte in a 3-electrode electrochemical cell setup with a CHI 760E potentiostat. A single yarn, an Ag/AgCl electrode, and a large-area Pt foil served as a working, a reference, and a counter electrode, respectively. Electrochemical impedance spectra (EIS) were measured at frequencies ranging from 0.01 to 100 000 Hz with a potential amplitude of 5 mV. All measurements were carried out at room temperature. Capacitances in the three-electrode cell were calculated according to ref 18. In brief, the capacitance of electrode ($C_{l,electrode}$) was calculated using the charge integrated from GCD and CV curves individually according to the formulas:

$$C_{l,electrode} = \frac{It}{U} \quad (1)$$

$$C_{l,electrode} = \frac{1}{2Uv}\int_{U_-}^{U_+} i(U)\,dU \quad (2)$$

where I is the discharge current during GCD, t is the discharge time during GCD, U is the voltage range ($U = U_+ - U_-$), v is the scan rate of the CV curve, and $i(U)$ is the current during CV. The yarn is approximately considered to be a cylinder. The surface area ($S_{electrode}$) and volume ($V_{electrode}$) of the yarn were determined according to the formulas:

$$S_{electrode} = \pi DL \quad (3)$$

$$V_{electrode} = \pi\left(\frac{D}{2}\right)^2 L \quad (4)$$

where D is the diameter of the yarn, and L is the length of the yarn. Specific capacitances normalized to length (C_L), area (C_A), and volume (C_V) were calculated by using the capacitance of electrode $C_{l,electrode}$ divided by the length L, area $S_{electrode}$, and volume $V_{electrode}$, individually.

Fabrication and Electrochemical Characterization of All-Solid-State Yarn Supercapacitors. PVA/H_3PO_4 electrolyte was prepared with 6 g H_3PO_4, 6 g PVA and 60 mL deionized water at 90 °C. Two identical as-deposited yarns were immersed in the cooled electrolyte solution for 5 min. Thereafter, the electrolyte wetted yarns were placed in parallel and dried until gel solidification under ambient conditions. Finally the solid-state supercapacitor was obtained with the electrolyte also serving as a separator. The performance of the assembled yarn supercapacitors was measured by CV and GCD in a two-electrode configuration using the potentiostat (CHI 760E). Capacitances, power and energy densities with respect to single electrode and the total volume/area of the device were individually calculated according to ref 18. In brief, the capacitance of the single electrode ($C_{s,electrode}$) was calculated using the charge integrated from GCD and CV curves individually according to the formulas:

$$C_{s,electrode} = \frac{2It}{U} \quad (5)$$

$$C_{s,electrode} = \frac{1}{Uv}\int_{U_-}^{U_+} i(U)\,dU \quad (6)$$

The capacitance of the device ($C_{s,device}$) is the half of $C_{s,electrode}$. The device is approximately considered to be a cubic. The energy density was obtained from the equation:

$$E = \frac{CU^2}{2 \times 3600} \quad (7)$$

where C is either $C_{s,electrode}$ (with respect to single electrode) or $C_{s,device}$ (with respect to device). The power density was calculated from the GCD curves by using the equation:

$$P = \frac{E \times 3600}{t} \quad (8)$$

Conflict of Interest: The authors declare no competing financial interest.

Supporting Information Available: Details of experimental methods, Supporting Information text, Figures S1−S12, Table S1 and references. This material is available free of charge *via* the Internet at http://pubs.acs.org.

Acknowledgment. This work was supported by the Early Career Scheme of the Research Grants Council of Hong Kong SAR, China (CityU 9041977) and the Science Technology and Innovation Committee of Shenzhen Municipality (JCYJ20130401145617276). The authors thank Z. P. Cheng, T. F. Hung, J. Yu, T. C. Lau and C. Huang for experimental support.

REFERENCES AND NOTES

1. Zeng, W.; Shu, L.; Li, Q.; Chen, S.; Wang, F.; Tao, X. M. Fiber-Based Wearable Electronics: A Review of Materials, Fabrication, Devices, and Applications. *Adv. Mater.* **2014**, *26*, 5310–5336.
2. Chen, T.; Dai, L. M. Carbon Nanomaterials for High-Performance Supercapacitors. *Mater. Today* **2013**, *16*, 272–280.
3. Sun, G. Z.; Liu, J. Q.; Zhang, X.; Wang, X. W.; Li, H.; Yu, Y.; Huang, W.; Zhang, H.; Chen, P. Fabrication of Ultralong Hybrid Microfibers from Nanosheets of Reduced Graphene Oxide and Transition-Metal Dichalcogenides and Their Application as Supercapacitors. *Angew. Chem., Int. Ed.* **2014**, *53*, 12576–12580.
4. Jung, H. Y.; Karimi, M. B.; Hahm, M. G.; Ajayan, P. M.; Jung, Y. J. Transparent, Flexible Supercapacitors from Nano-Engineered Carbon Films. *Sci. Rep.* **2012**, *2*, 773.
5. Kou, L.; Huang, T. Q.; Zheng, B. N.; Han, Y.; Zhao, X. L.; Gopalsamy, K.; Sun, H. Y.; Gao, C. Coaxial Wet-Spun Yarn Supercapacitors for High-Energy Density and Safe Wearable Electronics. *Nat. Commun.* **2014**, *5*, 3754.
6. Wang, X. B.; Zhang, Y. J.; Zhi, C. Y.; Wang, X.; Tang, D. M.; Xu, Y. B.; Weng, Q. H.; Jiang, X. F.; Mitome, M.; Golberg, D.; et al.

Three-Dimensional Strutted Graphene Grown by Substrate-Free Sugar Blowing for High-Power-Density Supercapacitors. *Nat. Commun.* **2013**, *4*, 2905.
7. Wang, X. F.; Liu, B.; Liu, R.; Wang, Q. F.; Hou, X. J.; Chen, D.; Wang, R. M.; Shen, G. Z. Fiber-Based Flexible All-Solid-State Asymmetric Supercapacitors for Integrated Photodetecting System. *Angew. Chem., Int. Ed.* **2014**, *53*, 1849–1853.
8. Cao, X. H.; Yin, Z. Y.; Zhang, H. Three-Dimensional Graphene Materials: Preparation, Structures and Application in Supercapacitors. *Energy Environ. Sci.* **2014**, *7*, 1850–1865.
9. Pushparaj, V. L.; Shaijumon, M. M.; Kumar, A.; Murugesan, S.; Ci, L.; Vajtai, R.; Linhardt, R. J.; Nalamasu, O.; Ajayan, P. M. Flexible Energy Storage Devices Based on Nanocomposite Paper. *Proc. Natl. Acad. Sci. U.S.A.* **2007**, *104*, 13574–13577.
10. Hu, L. B.; Pasta, M.; La Mantia, F.; Cui, L. F.; Jeong, S.; Deshazer, H. D.; Choi, J. W.; Han, S. M.; Cui, Y. Stretchable, Porous, and Conductive Energy Textiles. *Nano Lett.* **2010**, *10*, 708–714.
11. Jost, K.; Stenger, D.; Perez, C. R.; McDonough, J. K.; Lian, K.; Gogotsi, Y.; Dion, G. Knitted and Screen Printed Carbon-Fiber Supercapacitors for Applications in Wearable Electronics. *Energy Environ. Sci.* **2013**, *6*, 2698–2705.
12. Bao, L. H.; Li, X. D. Towards Textile Energy Storage from Cotton T-Shirts. *Adv. Mater.* **2012**, *24*, 3246–3252.
13. Liu, N. S.; Ma, W. Z.; Tao, J. Y.; Zhang, X. H.; Su, J.; Li, L. Y.; Yang, C. X.; Gao, Y. H.; Golberg, D.; Bando, Y. Cable-Type Supercapacitors of Three-Dimensional Cotton Thread Based Multi-Grade Nanostructures for Wearable Energy Storage. *Adv. Mater.* **2013**, *25*, 4925–4931.
14. Zhong, J. W.; Zhang, Y.; Zhong, Q. Z.; Hu, Q. Y.; Hu, B.; Wang, Z. L.; Zhou, J. Fiber-Based Generator for Wearable Electronics and Mobile Medication. *ACS Nano* **2014**, *8*, 6273–6280.
15. Shim, B. S.; Chen, W.; Doty, C.; Xu, C. L.; Kotov, N. A. Smart Electronic Yarns and Wearable Fabrics for Human Biomonitoring Made by Carbon Nanotube Coating with Polyelectrolytes. *Nano Lett.* **2008**, *8*, 4151–4157.
16. Zeng, W.; Tao, X. M.; Chen, S.; Shang, S. M.; Chan, H. L. W.; Choy, S. H. Highly Durable All-Fiber Nanogenerator for Mechanical Energy Harvesting. *Energy Environ. Sci.* **2013**, *6*, 2631–2638.
17. Xie, K.; Wei, B. Materials and Structures for Stretchable Energy Storage and Conversion Devices. *Adv. Mater.* **2014**, 3592–3617.
18. Yu, D. S.; Goh, K.; Wang, H.; Wei, L.; Jiang, W. C.; Zhang, Q.; Dai, L. M.; Chen, Y. Scalable Synthesis of Hierarchically Structured Carbon Nanotube-Graphene Fibres for Capacitive Energy Storage. *Nat. Nanotechnol.* **2014**, *9*, 555–562.
19. Lee, J. A.; Kim, Y. T.; Spinks, G. M.; Suh, D.; Lepro, X.; Lima, M. D.; Baughman, R. H.; Kim, S. J. All-Solid-State Carbon Nanotube Torsional and Tensile Artificial Muscles. *Nano Lett.* **2014**, *14*, 2664–2669.
20. Zhang, D. H.; Miao, M. H.; Niu, H. T.; Wei, Z. X. Core-Spun Carbon Nanotube Yarn Supercapacitors for Wearable Electronic Textiles. *ACS Nano* **2014**, *8*, 4571–4579.
21. Meng, Q. H.; Wu, H. P.; Meng, Y. N.; Xie, K.; Wei, Z. X.; Guo, Z. X. High-Performance All-Carbon Yarn Micro-Supercapacitor for an Integrated Energy System. *Adv. Mater.* **2014**, *26*, 4100–4106.
22. Meng, Q. H.; Wang, K.; Guo, W.; Fang, J.; Wei, Z. X.; She, X. L. Thread-like Supercapacitors Based on One-Step Spun Nanocomposite Yarns. *Small* **2014**, *10*, 3187–3193.
23. Lee, J. A.; Shin, M. K.; Kim, S. H.; Cho, H. U.; Spinks, G. M.; Wallace, G. G.; Lima, M. D.; Lepro, X.; Kozlov, M. E.; Baughman, R. H.; et al. Ultrafast Charge and Discharge Biscrolled Yarn Supercapacitors for Textiles and Microdevices. *Nat. Commun.* **2013**, *4*, 1970.
24. Zheng, B. N.; Huang, T. Q.; Kou, L.; Zhao, X. L.; Gopalsamy, K.; Gao, C. Graphene Fiber-Based Asymmetric Micro-Supercapacitors. *J. Mater. Chem. A* **2014**, *2*, 9736–9743.
25. Huang, T. Q.; Zheng, B. N.; Kou, L.; Gopalsamy, K.; Xu, Z.; Gao, C.; Meng, Y. N.; Wei, Z. X. Flexible High Performance Wet-Spun Graphene Fiber Supercapacitors. *RSC Adv.* **2013**, *3*, 23957–23962.
26. Xu, Z.; Gao, C. Graphene in Macroscopic Order: Liquid Crystals and Wet-Spun Fibers. *Acc. Chem. Res.* **2014**, *47*, 1267–1276.
27. Kou, L.; Liu, Z.; Huang, T.; Zheng, B.; Tian, Z.; Deng, Z.; Gao, C. Wet-Spun, Porous, Orientational Graphene Hydrogel Films for High-Performance Supercapacitor electrodes. *Nanoscale* **2015**, *7*, 4080–4087.
28. Lee, M. R.; Eckert, R. D.; Forberich, K.; Dennler, G.; Brabec, C. J.; Gaudiana, R. A. Solar Power Wires Based on Organic Photovoltaic Materials. *Science* **2009**, *324*, 232–235.
29. Pei, S. F.; Cheng, H. M. The Reduction of Graphene Oxide. *Carbon* **2012**, *50*, 3210–3228.
30. Chen, W.; Rakhi, R. B.; Hu, L. B.; Xie, X.; Cui, Y.; Alshareef, H. N. High-Performance Nanostructured Supercapacitors on a Sponge. *Nano Lett.* **2011**, *11*, 5165–5172.
31. Huang, Y.; Tao, J. Y.; Meng, W. J.; Zhu, M. S.; Huang, Y.; Fu, Y. Q.; Gao, Y. H.; Zhi, C. Y. Super-High Rate Stretchable Polypyrrole-Based Supercapacitors with Excellent Cycling Stability. *Nano Energy* **2015**, *11*, 518–525.
32. Yu, D. S.; Goh, K. L.; Zhang, Q.; Wei, L.; Wang, H.; Jiang, W. C.; Chen, Y. Controlled Functionalization of Carbonaceous Fibers for Asymmetric Solid-State Micro-Supercapacitors with High Volumetric Energy Density. *Adv. Mater.* **2014**, *26*, 6790–6797.
33. Bae, J.; Park, Y. J.; Lee, M.; Cha, S. N.; Choi, Y. J.; Lee, C. S.; Kim, J. M.; Wang, Z. L. Single-Fiber-Based Hybridization of Energy Converters and Storage Units Using Graphene as Electrodes. *Adv. Mater.* **2011**, *23*, 3446–3449.
34. Chen, T.; Qiu, L. B.; Yang, Z. B.; Cai, Z. B.; Ren, J.; Li, H. P.; Lin, H. J.; Sun, X. M.; Peng, H. S. An Integrated "Energy Wire" for Both Photoelectric Conversion and Energy Storage. *Angew. Chem., Int. Ed.* **2012**, *51*, 11977–11980.
35. Fu, Y. P.; Cai, X.; Wu, H. W.; Lv, Z. B.; Hou, S. C.; Peng, M.; Yu, X.; Zou, D. C. Fiber Supercapacitors Utilizing Pen Ink for Flexible/Wearable Energy Storage. *Adv. Mater.* **2012**, *24*, 5713–5718.
36. Ren, J.; Bai, W. Y.; Guan, G. Z.; Zhang, Y.; Peng, H. S. Flexible and Weaveable Capacitor Wire Based on a Carbon Nanocomposite Fiber. *Adv. Mater.* **2013**, *25*, 5965–5970.
37. Ren, J.; Li, L.; Chen, C.; Chen, X. L.; Cai, Z. B.; Qiu, L. B.; Wang, Y. G.; Zhu, X. R.; Peng, H. S. Twisting Carbon Nanotube Fibers for Both Wire-Shaped Micro-Supercapacitor and Micro-Battery. *Adv. Mater.* **2013**, *25*, 1155–1159.
38. Bae, J.; Song, M. K.; Park, Y. J.; Kim, J. M.; Liu, M. L.; Wang, Z. L. Fiber Supercapacitors Made of Nanowire-Fiber Hybrid Structures for Wearable/Flexible Energy Storage. *Angew. Chem., Int. Ed.* **2011**, *50*, 1683–1687.
39. Le, V. T.; Kim, H.; Ghosh, A.; Kim, J.; Chang, J.; Vu, Q. A.; Pham, D. T.; Lee, J. H.; Kim, S. W.; Lee, Y. H. Coaxial Fiber Supercapacitor Using All-Carbon Material Electrodes. *ACS Nano* **2013**, *7*, 5940–5947.
40. Jost, K.; Durkin, D. P.; Haverhals, L. M.; Brown, E. K.; Langenstein, M.; De Long, H. C.; Trulove, P. C.; Gogotsi, Y.; Dion, G. Natural Fiber Welded Electrode Yarns for Knittable Textile Supercapacitors. *Adv. Energy Mater.* **2015**, 10.1002/aenm.201401286.
41. Xu, J.; Wang, Q. F.; Wang, X. W.; Xiang, Q. Y.; Hang, B.; Chen, D.; Shen, G. Z. Flexible Asymmetric Supercapacitors Based upon Co_9S_8 Nanorod//Co_3O_4@RuO_2 Nanosheet Arrays on Carbon Cloth. *ACS Nano* **2013**, *7*, 5453–5462.
42. Sumboja, A.; Foo, C. Y.; Wang, X.; Lee, P. S. Large Areal Mass, Flexible and Free-Standing Reduced Graphene Oxide/Manganese Dioxide Paper for Asymmetric Supercapacitor Device. *Adv. Mater.* **2013**, *25*, 2809–2815.
43. Fu, Y. P.; Wu, H. W.; Ye, S. Y.; Cai, X.; Yu, X.; Hou, S. C.; Kafafy, H.; Zou, D. C. Integrated Power Fiber for Energy Conversion and Storage. *Energy Environ. Sci.* **2013**, *6*, 805–812.
44. Meng, Y. N.; Zhao, Y.; Hu, C. G.; Cheng, H. H.; Hu, Y.; Zhang, Z. P.; Shi, G. Q.; Qu, L. T. All-Graphene Core-Sheath Microfibers for All-Solid-State, Stretchable Fibriform Supercapacitors and Wearable Electronic Textiles. *Adv. Mater.* **2013**, *25*, 2326–2331.
45. Chen, X. L.; Qiu, L. B.; Ren, J.; Guan, G. Z.; Lin, H. J.; Zhang, Z. T.; Chen, P. N.; Wang, Y. G.; Peng, H. S. Novel Electric

Double-Layer Capacitor with a Coaxial Fiber Structure. *Adv. Mater.* **2013**, *25*, 6436–6441.
46. Wang, K.; Meng, Q. H.; Zhang, Y. J.; Wei, Z. X.; Miao, M. H. High-Performance Two-Ply Yarn Supercapacitors Based on Carbon Nanotubes and Polyaniline Nanowire Arrays. *Adv. Mater.* **2013**, *25*, 1494–1498.
47. Yuan, L. Y.; Yao, B.; Hu, B.; Huo, K. F.; Chen, W.; Zhou, J. Polypyrrole-Coated Paper for Flexible Solid-State Energy Storage. *Energy Environ. Sci.* **2013**, *6*, 470–476.
48. Yang, P. H.; Xiao, X.; Li, Y. Z.; Ding, Y.; Qiang, P. F.; Tan, X. H.; Mai, W. J.; Lin, Z. Y.; Wu, W. Z.; Li, T. Q.; et al. Hydrogenated ZnO Core-Shell Nanocables for Flexible Supercapacitors and Self-Powered Systems. *ACS Nano* **2013**, *7*, 2617–2626.
49. Lu, X. H.; Yu, M. H.; Wang, G. M.; Zhai, T.; Xie, S. L.; Ling, Y. C.; Tong, Y. X.; Li, Y. H-TiO_2@MnO_2//H-TiO_2@C Core-Shell Nanowires for High Performance and Flexible Asymmetric Supercapacitors. *Adv. Mater.* **2013**, *25*, 267–272.
50. Xiao, X.; Li, T. Q.; Yang, P. H.; Gao, Y.; Jin, H. Y.; Ni, W. J.; Zhan, W. H.; Zhang, X. H.; Cao, Y. Z.; Zhong, J. W.; et al. Fiber-Based All-Solid-State Flexible Supercapacitors for Self-Powered Systems. *ACS Nano* **2012**, *6*, 9200–9206.
51. Tao, J. Y.; Liu, N. S.; Ma, W. Z.; Ding, L. W.; Li, L. Y.; Su, J.; Gao, Y. H. Solid-State High Performance Flexible Supercapacitors Based on Polypyrrole-MnO_2-Carbon Fiber Hybrid Structure. *Sci. Rep.* **2013**, *3*, 2286.